ELEMENTA
Science of the Anthropocene

Riddick, SN, et al. 2022. A cautionary report of calculating methane emissions using low-cost fence-line sensors. *Elem Sci Anth*, 10: 1. DOI: https://doi.org/10.1525/elementa.2022.00021

RESEARCH ARTICLE

A cautionary report of calculating methane emissions using low-cost fence-line sensors

Stuart N. Riddick[1,*], Riley Ancona[1], Fancy Cheptonui[1], Clay S. Bell[1], Aidan Duggan[1], Kristine E. Bennett[1], and Daniel J. Zimmerle[1]

Methane (CH_4) is emitted during extraction, processing, and transport processes in the natural gas industry. As a powerful greenhouse gas, CH_4 releases are harmful to the environment. Operators aim to minimize methane loss, and continuous monitoring using low-cost fence-line sensors are now being developed to observe methane enhancements downwind of operations. However, it is not clear how useful these systems are and whether they can be used to quantify emissions or simply identify the presence of a leak. To investigate this, we deployed 4 calibrated low-cost sensors 30 m from emissions of known rates over a 48-h period. The aims were to determine: (1) how much of the time a fence-line system would detect a leakage event from a single, point source of the size typically seen at oil and gas production well pads and (2) how accurately a fence-line system can estimate CH_4 emissions using a relatively simple downwind dispersion method. Our results show that during a 48-h measurement period, the fence-line sensor network could detect CH_4 releases of 84 g h^{-1} 40% of the time and 100% of the time for emissions greater than 167 g h^{-1} using an enhancement threshold of 2 ppm. A Gaussian plume inversion based on binned centerline, maximum measured concentrations and the WindTrax Lagrangian particle model were each tested. With these models, average estimated emissions were within ±50% of a known emission rate in 24 h and ±25% in 48 h; however, estimated individual 20-min average emissions vary by more than a factor of 10. A simple Gaussian plume inversion using all of the measured concentrations produced unreasonable average emission estimates because of the inability of the equation to parameterize lateral dispersion at distances less than 100 m when the sensor was on the edge of the plume. This study provides evidence to support the use of low-cost sensors as autonomous fence-line monitoring systems to detect and potentially quantify emissions. If the sensors are properly calibrated and sensor deployment location is optimized for prevailing wind directions at each site, fence-line systems could be used routinely to quantify emissions from oil and gas infrastructure.

Keywords: Methane, Oil and gas extraction, Leakage, Detection, Emission estimate

1. Introduction

Methane (CH_4) is emitted during extraction, processing, and transport processes in the natural gas industry due to planned venting, unplanned fugitive releases, and as unburned CH_4 in combustion exhaust streams. As a powerful greenhouse gas and global ozone precursor, uncontrolled CH_4 releases are harmful to the environment and represent a loss to natural gas companies. Additionally, gas consumers and regulators are putting pressure on natural gas companies to reduce emissions, particularly of fugitive emissions, and provide certification of good practice. For example, legislation in the European Union's (EU) CH_4 strategy targets 55% reduction in CH_4 emissions by 2030, as compared to 1990 levels (EU, 2021), while certification includes the Natural Gas Supply Cooperative's certification process, Project Canary's TrustWell certification, and the Rocky Mountain Institute—SYSTEM-IQ's MiQ standard. It is therefore in the interests of oil and gas (O&G) operators to keep losses at a minimum.

The focus on fugitive emissions reduction has increased interest in advanced, or "next generation" methods for leak detection (Bell et al., 2020). These methods may be loosely grouped into 2 categories: (1) survey methods—a sensor or sensors are transported around a facility, collects data via one or more sensors, and analytics detect, and possibly quantify, from the facility, and (2) continuous monitoring—a set of sensors is installed on a facility more-or-less permanently and continuously—and likely autonomously—collects sensor data. These data are processed by analytics to detect, and possibly quantify, emissions from the facility.

In general, continuous monitors operate more of the time (daylight hours for some systems, continuously for others), allowing them to detect unexpected releases sooner than survey methods, which are typically scheduled on a monthly or less frequent basis. In contrast,

[1] The Energy Institute, Colorado State University, CO, USA

* Corresponding author:
Email: stuart.riddick@colostate.edu

survey methods can generally deploy more expensive sensors, and, by moving the sensor in an intelligent way, augment sensor readings with spatial data to improve detection probabilities.

Leak detector and repair (LDAR) methods are used by O&G operators to identify and correct upset emission conditions and can be classed as either in situ or downwind observations. In situ methods include observing the size of bubbles on leaking infrastructure (Log et al., 2019), Environmental Protection Agency's (EPA, 2021) Method 21, detecting emissions using optical gas imaging cameras (Bell et al., 2017; Log et al., 2019; Zimmerle et al., 2020), and hi-flow sampling (Bell et al., 2017; Riddick et al., 2022). The main advantage of in situ measurements is that the instruments are relatively cheap. The shortcomings are they can take a long time to do, are survey methods, and require relatively skilled operators (Zimmerle et al., 2020).

Downwind methods include the U.S. EPA's Other Test Method (OTM) 33A (Bell et al., 2017; Edie et al., 2020), using point source sensors (Riddick et al., 2020), using line averaged open-path lasers (Alden et al., 2018; Alden et al., 2019), tracer flux methods (Lamb et al., 1995; Allen et al., 2015; Vaughn et al., 2017), and aircraft-based mass balance methods (Conley et al., 2017; Duren et al., 2019). Downwind measurements can have high detection limits and may not detect smaller emissions (especially aircraft based methods), require expensive gas analyzers/lasers to measure trace gas concentrations, are mostly survey methods, and require expertise to run. The advantage of the downwind methods is that most are quick at measuring facility emissions, and many sites can be measured in a relatively short time.

Of the methods listed above, only the point source sensors and line averaged open-path lasers are routinely used as continuous monitors. The advantage of continuous monitoring is that it can be used to observe temporal changes in emission and are more likely to detect and possibly quantify short, periodic emissions. Open-path lasers can measure CH_4 enhancements up to 1 km away from the emission source and have been reported to measure emissions as low as 58 g CH_4 h^{-1} at this distance (Alden et al., 2019). Their main shortcoming is cost and a system that could be used to monitor multiple well pads up to 1 km away costs more than $100 k. Point source sensors are lower cost, but sensitivity and response to CH_4 varies between individual sensors (Eugster and Kling, 2012; Riddick et al., 2020); they are fixed in one location and will only detect an emission if the plume passes over the sensors. The detection limit of point source sensors is currently unclear.

There is a growing interest in the deployment of one or more relatively low-cost concentration sensors on the edge, or "fence-line," of a facility. U.S. state regulators, including Colorado, are in the early stages of requiring continuous monitoring of O&G sites, starting with preproduction (drilling) sites (Colorado Department of Public Health and Environment [CDPHE], 2021a), and the trend is being further encouraged by the development of a new generation of more stable low-cost ($10 s) sensors. Fence-line monitoring uses multiple instruments fixed at the boundary of O&G operations to continuously measure gas concentrations. If the measured gas concentrations downwind of a source are sufficiently higher than the background concentration for a set predefined period, an emission is detected, and the operator is alerted. Currently, there are no published studies investigating the use of fence-line systems to monitor/quantify CH_4 emissions from O&G production well pads.

Unlike natural CH_4 sources, such as wetlands, that emit gas in response to changes in environmental conditions, O&G production sites emit CH_4 when pieces of equipment either vent or fail, and emissions can happen at various stages of production. Taking a wet gas production site as an example (**Figure 1**), mixed phase product is extracted from the ground when the well head is opened and closed usually using natural gas powered pneumatics. The produced condensate, water and natural gas is separated in stages, and natural gas is exported for further refinement via gathering lines. Gas in the lower pressure second and third stages of separation requires repressurization using vapor recovery units (VRUs). Produced water and gas are generally stored in tanks and transported for processing via trucks depending on the production rate and the size of the tanks.

On each well pad, there are thousands of components, including flanges, valves, and connectors, each of which is a possible emission source. Well pad areas range in size from hundreds to thousands of square meters. Methane emission can occur through controlled venting or during an upset condition. Typical vented emissions are the natural gas pneumatics found on the well heads, maintenance emissions (e.g., VRU blowdown and restart), gas slip from the VRUs, venting when the VRUs are overwhelmed, and incomplete combustion of gas by the flare. Flare destruction efficiency is generally accepted to be 98% but has been observed as low as 55% (Johnson and Kostiuk, 2002; Chambers, 2003; Johnson et al., 2017; Zavala-Araiza et al., 2021).

Upset conditions that result in uncontrolled release of CH_4 include stuck dump valves, VRU failure, flare outage, leakage from either the flowline (well head to separator) or gathering line (well pad to export), and thief hatches on the water/condensate tanks left open. The EPA define a leak as an emission where the measured CH_4 concentration in air exceeds a threshold standard, where the lowest threshold from National Emission Standards for Hazardous Air Pollutants is 500 ppm (EPA, 2021). Unloading of water and condensate to trucks is another source of CH_4 emission, but more sophisticated systems now use vapor return lines from the tanker to the tanks to reduce emissions.

Methane will be emitted at O&G facilities either through venting or leakage, and it is incumbent on the O&G operators to reduce the emissions, with the prime driver being regulation. Regulation varies both internationally and regionally. Some countries require O&G operators to provide annual estimates for the flaring/venting volumes, have a clear government policy for flaring and venting, and a governmental regulatory body overseeing overall emission targets, legislation, regulation, and monitoring strategies. Most other countries have venting

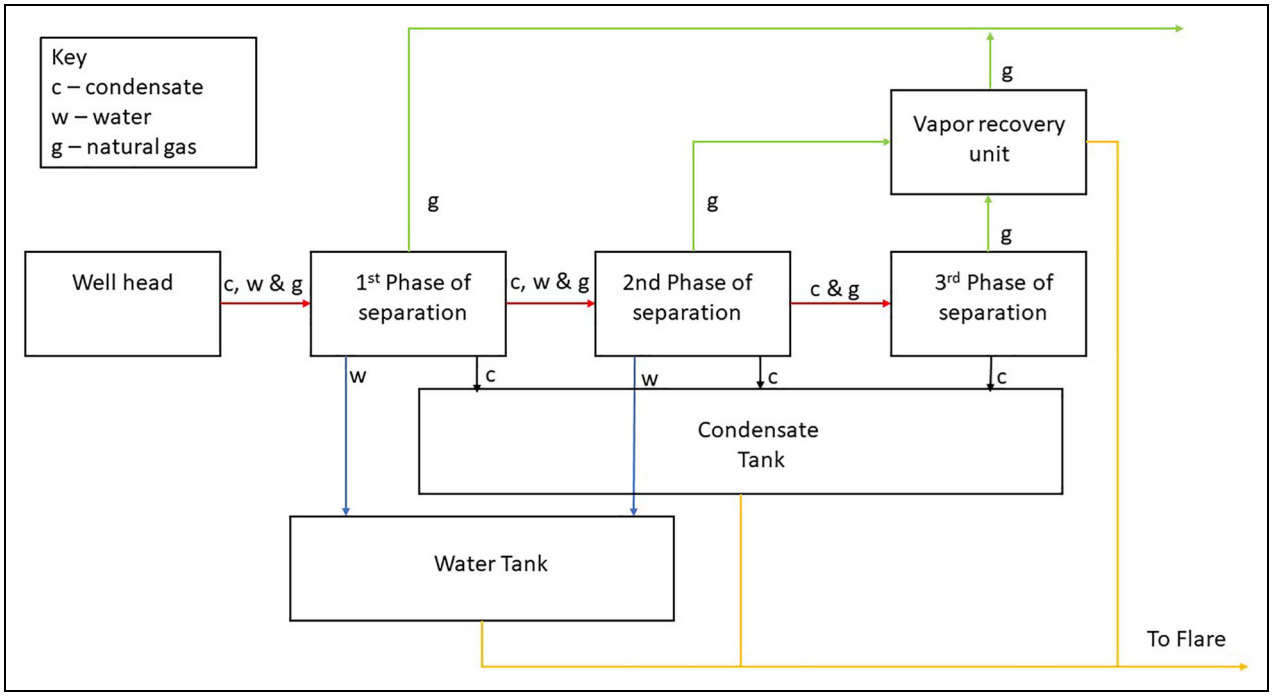

Figure 1. Schematic of the major pieces of equipment at a wet gas oil and gas facility, where c denotes the flow of condensate, w denotes water, and g denotes the flow of natural gas. DOI: https://doi.org/10.1525/elementa.2022.00021.f1

and flaring regulations, but gas from process and combustion activities can be vented to the atmosphere without regulation (World Bank Group, 2013; 2021). It is currently unclear how successful regulation is because in most cases, compliance does not require verification through measurement. New initiatives, such as the Approved Instrument Monitoring Method in Colorado, require operators to inspect components using methods with rigorously tested detection limits (CDPHE, 2021b).

Despite advancements in technology, it remains unclear how well a fence-line system can detect/quantify leaks from O&G production well pads and how quickly this system can report a leak after it has started. Concentrations downwind of a point source, as might be expected from an individual leak on equipment on a well pad, are affected by the size of the leak and the meteorological conditions, and the likelihood of detection will also depend on these. If a leak occurs directly upwind of a sensor during a constant wind, it is reasonable to expect it to be detected very quickly. However, in a variable wind, it is likely that the gas plume will not remain centered on the sensor, and the concentration will fluctuate, at times, rapidly. Also, in low, unstable winds with a lot of vertical gas transport, it is possible that the plume could pass over the top of the sensors, and the leak remains undetected.

In addition to on-site monitoring, similar sensors have been proposed for community monitoring of O&G facilities, with some active deployments looking at both CH_4 and volatile organic compounds in communities adjacent to O&G facilities (Clements et al., 2017; Collier-Oxandale et al., 2018; Morawska et al., 2018; Shamasunder et al., 2018; Okorn et al., 2021). In general, this application is further downwind of emission points and therefore likely sensing lower concentrations of pollutants. However, community groups are often more cost-sensitive than O&G operations and therefore driven toward low-cost sensors and deployment options. These performance questions are therefore of interest not only to O&G operations but to community groups impacted by these operations.

Thus, in this study, we investigate the ability of fence-line monitors to detect a leak. Using point sources of known emission rates, our aims were to determine (1) how much of the time a common fence-line strategy would detect a leakage event from a single, point source of the size typically seen at O&G production well pads and (2) how accurately a fence-line system can estimate emissions using a relatively simple downwind dispersion method.

2. Materials and methods

2.1. Controlled emission methodology

2.1.1. Fence-line deployment

A simulated fence-line was constructed at the Colorado State University Methane Emissions Technology Evaluation Center (METEC) site in Fort Collins, CO, USA, between August 27 and September 4, 2020 (**Figure 2**). Four Figaro TGS2611-E00 sensors (Figaro Engineering, Inc., Osaka, Japan) were deployed with control from a Raspberry Pi and power supplied by solar panels. The sensors were mounted in holes in the bottom of a weather-resistant box and exposed to sample air passing the bottom of the box. Each sensor box also contained a DHT22 temperature and relative humidity sensor (Adafruit Industries, New York, NY, USA).

Each sensor box was calibrated (details in Text S2), mounted on a moveable mast 1.2 m above the ground and 30 m from the emission point. The 30 m distance was

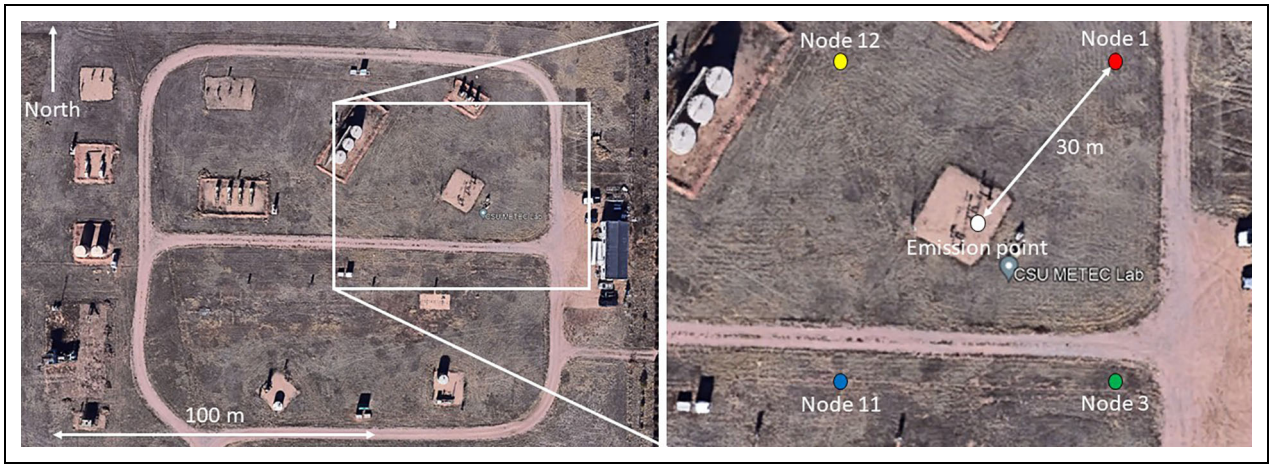

Figure 2. Location of fence-line sensors. Deployment locations of the 4 measurement nodes (Nodes 1, 3, 11, and 12) at the Colorado State University Methane Emissions Technology Evaluation Center site in Fort Collins, CO, USA, between the 27 August and 4 September, 2020. Map from Google Maps: www.google.com/maps. DOI: https://doi.org/10.1525/elementa.2022.00021.f2

based on Section 602, subsection (f) of the 600 Series safety rules from the Colorado Oil and Gas Conservation Commission (2020), where vehicles must be at least 30 m from the well bore. The sensors were placed orthogonally and in line with the most likely wind directions (WDs) to detect enhancements, where the prevailing winds at METEC are either from the southeast or the northwest (**Figure 1**; right panel).

2.1.2. Controlled emissions

METEC can reproduce constant CH_4 emissions from 20 g CH_4 h^{-1} to 40 kg CH_4 h^{-1} which are representative of those typically seen from individual point sources at O&G operations (Allen et al., 2013; Allen et al., 2015; Bell et al., 2017; Pacsi et al., 2019). Release points are located on realistic equipment, in locations where component leaks are commonly seen on well pads and similar O&G infrastructure. For the purposes of this study, where we investigated the ability of a fence-line system to detect an emission from a point source, CH_4 emission rates of 84, 167, and 313 g CH_4 h^{-1} were run for 48-h each. These emission values were chosen as the 25th, 50th, and 75th percentile of leak size observed during measurement campaigns at natural gas production sites in the United States, not including liquid unloading events (Allen et al., 2013; Allen et al., 2015; Bell et al., 2017; Pacsi et al., 2019) or major abnormal process conditions, such as stuck dump valves in separators or unlit flares.

2.2. Detection events

Methane mixing ratios in air were measured by the calibrated TGS2611 sensors collecting data every 5s. Three detection event experiments were conducted to determine the fraction of time that measured mixing ratios were larger than a defined mixing ratio threshold. Figaro sensors were observed to drift by 0.002 ppm day^{-1} (Riddick et al., 2020) and to account for any drift the enhanced mixing ratio was reported instead of the absolute mixing ratio. Enhancements in this case are the background CH_4 mixing ratio subtracted from the downwind CH_4 mixing ratio, where the background is calculated as the 5th percentile mixing ratio over a rolling 4-h period to capture intermittent enhancements from other sources in the "background" measurement. Fixed enhancement threshold values used were 0.2, 2, 3, 5, and 7 ppm. The 3 experiments were as follows:

Scenario 1—Calculate average mixing ratios over a range of fixed periods of time and report the average mixing ratio after every calculation. Fixed periods were 5 s, 10 s, 30 s, 1 min, 5 min, 10 min, and 20 min.

Scenario 2—Calculate running average mixing ratios over a range of fixed periods and report the running average every 5s. Fixed periods were the same as Scenario 1.

Scenario 3—Turn sensors on and off to conserve energy. Calculate a 5-min averaged mixing ratio for sensors that turn on every 5s, 10s, 30s, 1 min, and 5 min.

2.3. Estimating emissions

The CH_4 emissions were calculated using CH_4 mixing ratio enhancements and matching meteorological data using 3 approaches: (1) a simple Gaussian plume (GP) equation; (2) downwind GP equation, and (3) a backward Lagrangian stochastic (bLs) model. In each case, the 48-h average emissions are calculated for the 3 release rates and presented with matching uncertainty bounds.

In addition to CH_4 mixing ratio data, meteorological data are required as input. Wind speed and direction were measured every 30 s using a Kestrel 5500 weather meter (Kestrel Instruments, Boothwyn, PA, USA) on a mast 1.5 m above the ground. To reduce any impact of mechanical turbulence while maintaining real changes to CH_4 emission caused by changing environmental or atmospheric factors, both CH_4 mixing ratio and meteorological data were averaged over a 20 min interval to minimize any effects of

turbulence while preserving variation caused by environmental or atmospheric change (Laubach et al., 2008; Flesch et al., 2009). Figaro TGS sensors do not work reliably in low humidity conditions (Eugster and Kling, 2012; Riddick et al., 2020), and 20-min averaged data were removed for measurements made in a relative humidity of less than 30%. The Pasquill–Gifford stability class (PGSC) during each measurement was calculated from meteorological data using the lookup table in Table S2 (Pasquill, 1975; Pasquill and Smith, 1983; Seinfeld and Pandis, 2016).

2.3.1. Approach 1—The GP equation

This approach was chosen for testing because of its ease of application. The GP equation is relatively straightforward, using an algorithm to calculate the emission rate. The simplicity of the approach allows emissions to be calculated in real time. The GP equation describes the concentration of a gas as a function of distance downwind from a point source (Seinfeld and Pandis, 2016). As gas is emitted from a source, it is entrained in the prevailing ambient air flow and disperses laterally and vertically with time, forming a dispersed concentration cone. The mixing ratio enhancement (X, μg m^{-3}), at any point x m downwind of the source, y m laterally from the center line of the plume and z m above ground level can be calculated using the emission rate (Q_e, g s^{-1}), the wind speed (U, m s^{-1}), the WD (°) the height of the source (h_s, m) and the PGSC as a measure of air stability (Equation 1).

$$X(x,y,z) = \frac{Q_e}{2\pi U \sigma_y \sigma_z} e^{-\frac{y^2}{(2\sigma y)^2}} \left(e^{-\frac{(z-h_s)^2}{(2\sigma_z)^2}} + e^{-\frac{(z+h_s)^2}{(2\sigma_z)^2}} \right). \quad (1)$$

The standard deviation of the lateral (σ_y, m) and vertical (σ_z, m) mixing ratio distributions is calculated from the PGSC of the air (Busse and Zimmerman, 1973; U.S. EPA, 1995). The GP equation assumes that the vertical eddy diffusivity and wind speed are constant, and there is total reflection of CH_4 at the ground surface. For the GP method, including emission estimates when the sensor is on the edge of the plume yields unreasonable errors and an error limit of 5 times (500%) the known emission rate is imposed. Average emission and ranges are then reported using these filtered data.

2.3.2. Approach 2—The central GP (cGP) equation

Following the approach of Peterson and Lamb (1992), the cGP uses many of the advantages of the GP equation, such as simplicity and near-real time calculations, but avoids some of the shortcomings, such as knowing exactly where you are in the plume. Here, the cGP equation assumes that the highest concentrations will be detected directly downwind of the source and avoids the inclusion of the lateral dispersion as y is equal to zero. For each sensor, the mixing ratio time series was binned by 5° WD sectors and the mixing ratios in the bin with the highest concentrations used for inverse modeling (Peterson and Lamb, 1992).

2.3.3. Approach 3—The bLs approach

A bLs approach models the movement of a gas in the atmosphere travelling between a source and detector (Flesch et al., 1995; Flesch et al., 2005). Simulations model the trajectory of thousands of CH_4 particles as aerodynamic forces in the boundary layer act upon them. Each bLs simulation determines the ratio of the expected measured concentration and emission rate in prescribed meteorological and micrometeorological conditions and scales this to the measured mixing ratio enhancement (Flesch et al., 1995; Flesch et al., 2005; Flesch et al., 2009).

In this study, WindTrax version 2.0.8.8 (Flesch et al., 1995) was used in inverse mode to infer the CH_4 emissions from a point source. Each of the averaged enhancements were used as input data to back-calculate the CH_4 emission using 50,000 particle projections. Data used as input to WindTrax are U, WD, T, X, and PGSC. The roughness length was estimated from observation of the fetch and estimated to be short grass, where $z_0 = 2.3$ cm.

3. Results

3.1. Meteorological data

Between 1900 UTC on August 27 and 1400 UTC on September 2, 2020, air temperature measured at 7 m above the ground varied from 9.7°C to 31.9°C, while the relative humidity varied from 9% to 99% (**Figure 3A**). Both air temperature and relative humidity had strong diurnal cycles. Wind speed varied between 0 and 6.1 m s^{-1} and was predominantly from the south (**Figure 3B**).

3.2. Detection of CH_4 enhancements

Four TGS2611-E00 sensors were deployed concurrently with meteorological detection devices. The data from the sensors were converted to mixing ratios, as described in Text S1, and calculated mixing ratios ranged from 0.79 to 655 ppm during the measurement period. The 48-h average mixing ratios were 2.85, 7.5, and 9.0 ppm for the 84, 167, and 313 g CH_4 h^{-1} releases, respectively (**Figure 4**).

For a fence-line system calculating fixed time averages, increasing the averaging time increases the probability that at least one of the sensors will be above the threshold value (Table S3). The 20-min averaged enhancement mixing ratios were larger than the mixing ratio enhancement thresholds (0.2, 2, 3, 5, and 7 ppm) for a 167 and 313 g CH_4 h^{-1} emission all of the time, while a 1-min average detected a 167 g CH_4 h^{-1} emission 42% of the time with a 5 ppm enhancement threshold and 13% of the time with a 7 ppm enhancement threshold. All time averages will detect a 167 and 313 g CH_4 h^{-1} emission at least 25% of the time. To detect an 84 g CH_4 h^{-1} emission, all time averages could be used equally well, approximately 40% of the time, with an enhancement threshold of 2 ppm. All other mixing ratio enhancement thresholds will detect this emission less than 6% of the time.

For running averages, the length of averaging time does not make a difference to the fraction of time the emission is detected (Table S4), but the amount of time that the sensors detected the emission decrease as the mixing ratio enhancement threshold increases. For example, the sensor array will detect 167 g CH_4 h^{-1} emissions 100% time with a 3 ppm enhancement threshold, approximately 50% of the time with a 5 ppm threshold and approximately 25% of the time with a 7 ppm

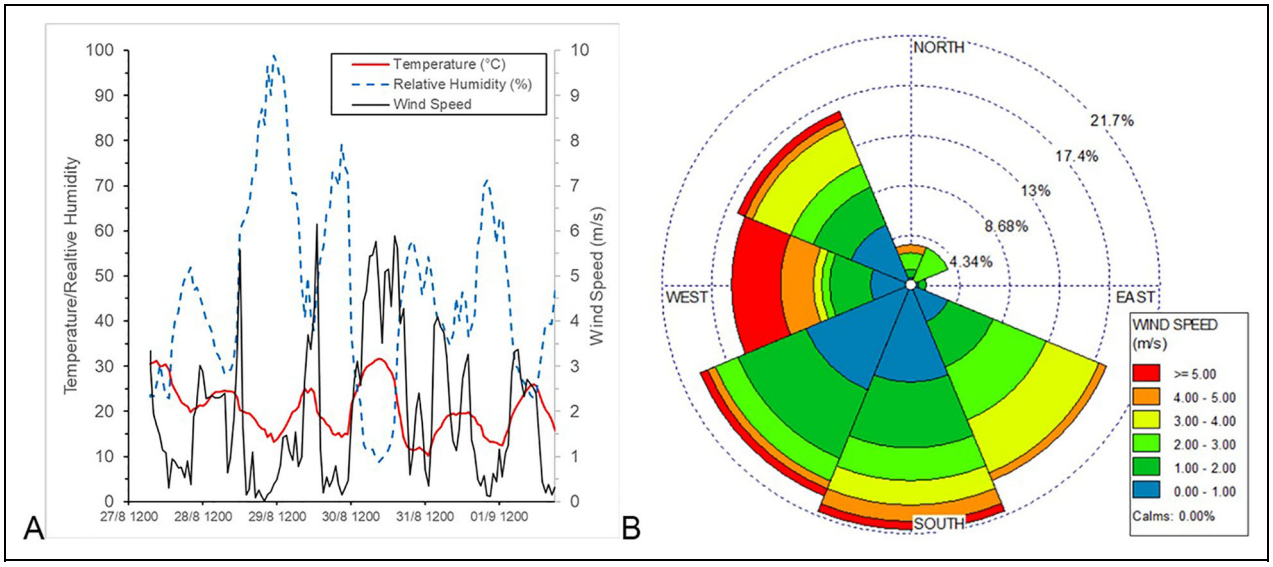

Figure 3. Meteorological data during emissions. (A) Wind speed, temperature, and relative humidity measured at Methane Emissions Technology Evaluation Center (METEC) between 1900 UTC on the August 27 and 1400 UTC on September 2, 2020. (B) Wind speed rose as measured at METEC between the same dates. DOI: https://doi.org/10.1525/elementa.2022.00021.f3

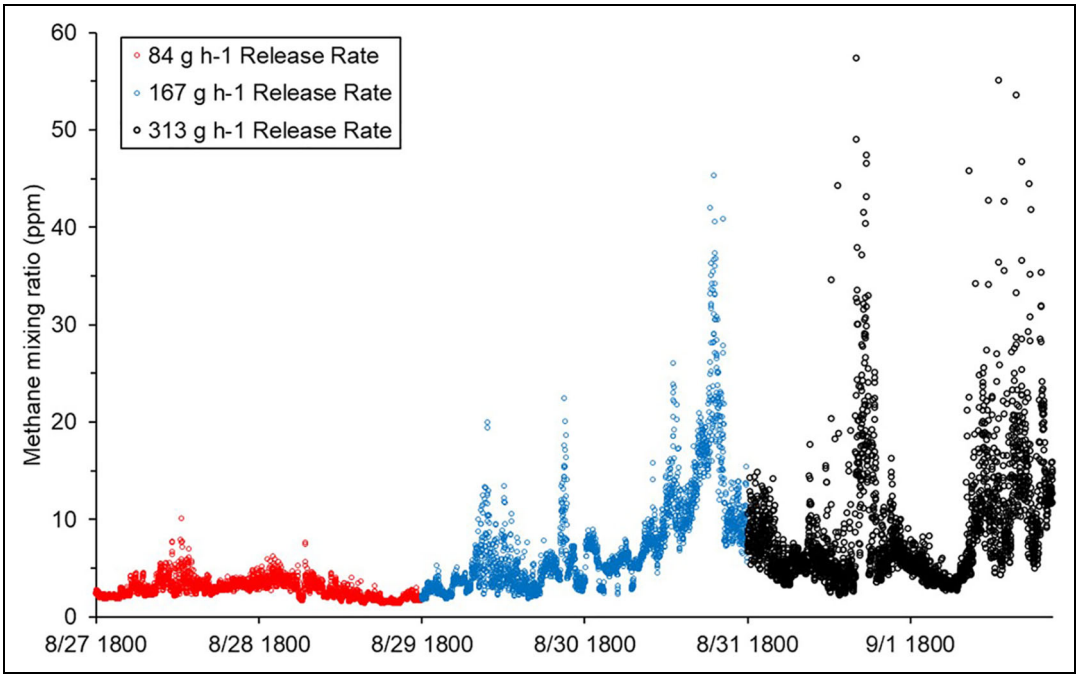

Figure 4. Downwind mixing ratios measured during releases. Downwind 5-s mixing ratios detected by the fence-line sensor nodes during the 84, 167, and 313 g CH_4 h^{-1} emission events. DOI: https://doi.org/10.1525/elementa.2022.00021.f4

enhancement threshold. A 2 ppm enhancement threshold will detect 84 g CH_4 h^{-1} emission approximately 40%, and all other mixing ratio thresholds will detect this emission less than 6% of the time.

For sensors turning on and off, the data show it does not make a difference how often they are turned on and off (Table S5). For the 167 g CH_4 h^{-1} emission, the sensors were above the 3 ppm enhancement threshold 100% of the time, approximately 60% of the time with a 5 ppm enhancement threshold and approximately 25% of the time with a 7 ppm enhancement threshold regardless of whether the sensor was turned on once every 5 s or 5 min. For 84 g CH_4 h^{-1}, the 2 ppm enhancement threshold will detect emission approximately 15%, and all other mixing ratio enhancement thresholds will detect the emission less than 2% of the time.

Table 1. Comparison of 48-h average emission for the Gaussian Plume (GP), central Gaussian Plume (cGP), and backward Lagrangian stochastic (bLs) approaches. DOI: https://doi.org/10.1525/elementa.2022.00021.t1

Method	48-h Average Emission (g h^{-1})	Range (%)	48-h Average Emission (g h^{-1})	Range (%)	48-h Average Emission (g h^{-1})	Range (%)
Known	84		167		313	
GP	12	−100, +500	26	−100, +500	122	−100, +500
cGP	71	−100, +359	177	−100, +802	386	−100, +860
bLs	86	−100, +805	191	−100, +1,885	367	−100, +946

Range presents the range of uncertainties individual measurements can be from the average emissions presented as an uncertainty.

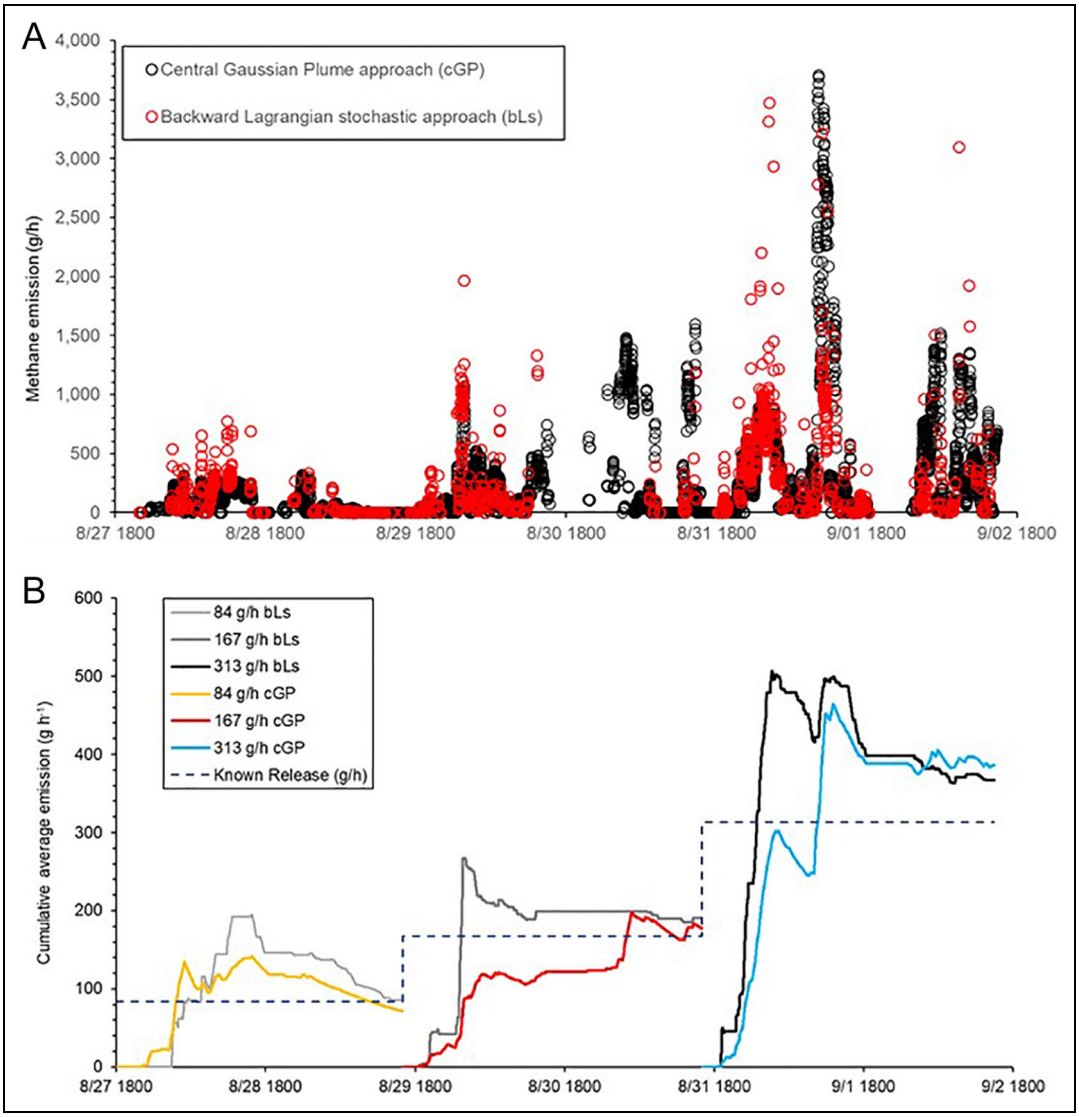

Figure 5. (A) Emissions calculated using the downwind Gaussian Plume (GP) equation and backward Lagrangian stochastic (bLs) model. (B) Cumulative average emissions using the downwind GP equation and bLs model data. DOI: https://doi.org/10.1525/elementa.2022.00021.f5

3.3. Calculating CH_4 emissions using fence-line measurements

Methane mixing ratio data and matching meteorological–micrometeorological data were input to the GP equation (Equation 1), filtered for an error limit of 5 times (500%) the known emission rate, and average emissions were calculated at 12, 26, and 122 (all g CH_4 h^{-1}) for the 84, 167, and 313 g CH_4 h^{-1} releases, respectively (**Table 1**).

Using the cGP approach, the average calculated emissions were 71, 177, and 386 (all g CH_4 h^{-1}) for the 84, 167,

and 313 g CH_4 h^{-1} releases, respectively (**Table 1**). The minimum uncertainty in an individual measurement in all cases was −100%, while the maximum uncertainty in an individual measurement was +359%, +802%, and +860% for the 84, 167, and 313 g CH_4 h^{-1} releases, respectively (**Figure 5**).

Using the bLs approach, the average calculated emissions were 86, 191, and 367 (all g CH_4 h^{-1}) for the 84, 167, and 313 g CH_4 h^{-1} releases, respectively (**Table 1**). Minimum uncertainty in individual measurements was −100%, and the maximum uncertainty was +805%, +1,885%, and +946% for the 84, 167, and 313 g CH_4 h^{-1} releases, respectively (**Figure 5**).

For both the cGP and bLs approaches, the cumulative average emissions converged to ±50% of the known release rate within 24 h (**Figure 5B**). For the 84 and 167 g CH_4 h^{-1} emissions, the cumulative average emission converges on the known emission to within ±15% of the known release rate within 48 h. The emission estimate for the 313 g CH_4 h^{-1} for both the cGP and bLs approaches remains at +25% of the known release rate after 48 h.

4. Conclusions

4.1. Leak detection

This study investigated the use of low-cost sensors to detect of CH_4 leakage from O&G infrastructure and calculate emission rates. All tests were done in a controlled environment where only 1 emission point was active, and the point was exactly known; there was no uncertainty in the location, rate, and positioning of the sensor relative to the emission point. Therefore, these tests represent an upper bound on the accuracy and utility of this type of sensor.

When deployed as described earlier, the sensors reported CH_4 mixing ratios from 0.79 to 39.1 ppm during the measurement period. The lower end of this range, below the expected background of 1.92 ppm, coincided with periods where the relative humidity was less than 30%, and the sensors report highly inaccurate readings in line with previous studies (Eugster and Kling, 2012; Riddick et al., 2020). This highlights one of the major shortcomings of using low-cost sensors for fence-line monitoring: Instabilities in the sensor reduce periods when reliable information can be collected.

Another shortcoming of using low-cost sensors for leak detection is that each individual sensor needs to be individually calibrated. Each TGS2611-E00 sensor responds differently to changes in CH_4 concentration (Table S1), requiring independent calibration against the range of concentrations observed in the field using a high precision trace gas analyzer, while controlling key environmental parameters, such as humidity.

Results of 3 experiments demonstrate the utility of detection strategies: Scenario 1—Calculate average mixing ratio enhancements over a range of fixed periods of time, Scenario 2—Calculate running average mixing ratio enhancements, and Scenario 3—Calculate a 5-min averaged mixing ratio enhancement for sensors that turn on every 5 s, 10 s, 30 s, 1 min, and 5 min. For the medium (167 g CH_4 h^{-1}) and large (313 g CH_4 h^{-1}) emissions, there does not seem to be a preferable strategy. In all 3 strategies, mixing ratio enhancement thresholds of 2 ppm and 3 ppm were exceeded by one of the sensors 100% of the time. For the 84 g CH_4 h^{-1} emission rate, only a 2 ppm enhancement threshold will result in a detection, and Scenarios 1 and 2 detected emissions twice as often as Scenario 3. In conclusion, it does not seem to matter what approach is used as the results for each are relatively similar. Interestingly, results from the on/off approach do not seem to affect the detection capabilities of the system, and a sensor system that takes a measurement every 5 min is only half as good as a system measuring and reporting mixing ratios every 5 s. A caveat should be added that these are the results from a continuously running system, and the outcomes may be different from an intermittent emission source.

An improvement to low-cost sensing deployment could be using multiple, colocated sensors to generate an average mixing ratio between the sensors and give more confidence to the mixing ratio measurements. The shortcoming of this is that 2 sensors require twice as much power, and in many deployments, low power is as important as low cost. Care should be taken when identifying a site-specific event threshold as background emissions from neighboring sites or from process vents on the facility could reach these concentrations depending on the proximity and location of the background sources, especially of a relatively low threshold (3 ppm) is chosen. An appropriate event threshold that will minimize false positive indications while still providing enough sensitivity to identify emission sources consistent in rate with those observed in leak surveys will prove difficult to establish.

4.2. Quantifying emissions

Using this fence-line approach presents an attractive option for O&G companies to continuously measure leakage rates remotely. A simple GP inversion using all of the measured concentrations produced unreasonable average emission estimates because of the inability of the equation to parameterize lateral dispersion at distances less than 100 m when the sensor was on the edge of the plume. This highlights the biggest issues with the GP equation: It lacks internal quality controls which evaluate inputs and signal if input data are insufficient to produce an accurate result.

Using an alternative method that has either internal (bLs) or forced (cGP) checks on whether the detector can realistically detect the plume at a distance downwind can result in the calculation of representative emission estimates. The bLs approach models the random-walk path of particles from source to detector, and measurements are rejected ("emission = –9,999" in model output) when it is infeasible that a detector will observe an emission from the source. Similarly, the data selection method used in the cGP approach discards measurements where concentrations are low. The bLs averaged emissions are higher than the cGP (**Figure 5A** and **B**), which may be an artifact of the directional nonfiltering in the bLs approach where, similar to the GP approach, large emissions caused by

measurement on the edge of the plume can be retained in the data set.

The main shortcoming of the cGP method is that a representative amount of mixing ratio data must be collected and processed before being binned by wind direction and the most suitable bin used in the analysis. Unlike the cGP, the bLs can run in near real time and calculate emissions as data are collected. The shortcoming of the bLs is that the uncertainty bounds of individual measurements are much larger (approximately factor of 2) than individual measurements of the cGP. Despite this, the cumulative average emission calculated using the cGP and bLs approaches is within $\pm 50\%$ of the known release rate within 24 h and $\pm 25\%$ after 48 h (**Figure 5B**).

The major assumption used in these analyses is that the location of the emission point is known. In an actual deployment, the location of the emissive part of equipment is generally unknown, even though the location of some sources such as vents and pressure relief valves will be known and must be estimated prior to employing a method to estimate the emission rate. Locating the source in *x*, *y*, *z* space is typically accomplished by observing elevated mixing ratios from multiple sensors and using wind direction to estimate possible origin points. This method requires wind directions to vary substantially (or many fence-line monitors) and has substantial location errors. At the largest sites, there are thousands of possible emission points on well pads spread over square kilometer, which may be further screened/confounded by emitting vents. The challenge of localization is nontrivial, and it is unclear whether it can be accomplished using low-cost sensors. Lack of an accurate leak position injects an additional challenge into fence-line monitoring in general and into employing a low-cost sensor for these systems.

4.2. Community monitoring

Results developed here indicate that community monitoring efforts should proceed with caution despite positive results reported in some recent studies (Collier-Oxandale et al., 2018; Okorn et al., 2021), as these systems are further from sites and often with less knowledge of potential sources of emissions. From a practical standpoint, current low-cost sensors also present deployment challenges for nonscientists, including calibration and filtering data for meteorological conditions incompatible with the sensors' capabilities (humidity) or simple emission rate estimation methods (stability and wind speed).

4.3. Future directions

There is some evidence that new types of low-cost sensors may reach the market in 1–3 years, potentially improving the stability of low-cost sensors and possibly improving the response or accuracy at the low mixing ratios seen in fence-line monitoring. While this would reduce the need to calibrate individual sensors, and potentially support quality output at low relative humidity, the requirements to filter the data and estimate the location of the emission point are unlikely to change.

The analysis presented here uses an uncomplicated GP equation with very simplified approximations for the micrometeorology, that is, the PGSC. It is possible that more complex dispersion modeling, such as computation fluid dynamics, for example, Sonderfeld et al. (2017), could be developed and integrated with in situ data collection software to provide real-time emissions from more wind directions.

If the caveats of calibration are addressed, modeling is improved, and deployment location is optimized for each site, there is reason to believe that fence-line systems could be used routinely to detect fugitive emissions from O&G infrastructure. This would inform leak and detection programs across the world and improve response time to isolate and repair leaks. It is less clear whether the same sensors will be capable of generating quantified estimates of emissions, or whether those estimates can handle the highly variable emissions often seen at O&G facilities. Considering both detection and quantification, care should be taken to not blindly adopt low-cost continuous monitors as a replacement of existing LDAR methods, or to blindly trust quantification estimates from these systems due to the practical limitations associated with the high spatial and temporal variability of O&G emissions.

Data accessibility statement

Data can be accessed at https://mountainscholar.org/handle/10217/234550.

Supplemental files

The supplemental files for this article can be found as follows:

Figures S1 and S2, Text S1 and S2, and Tables S1–S5. Docx

Funding

This work was funded by the METEC Industry Advisory Board (IAB) at Colorado State University.

Competing interests

The authors declare that no financial interest or benefit that has arisen from the direct applications of this research.

Author contributions

- Contributed to conception and design: SNR, RA, CSB, DJZ.
- Contributed to acquisition of data: SNR, RA, AD, CB.
- Contributed to analysis and interpretation of data: SNR, RA, FC.
- Drafted and/or revised the article: SNR, RA, FC, CSB, KEB, DJZ.
- Approved the submitted version for publication: SNR, RA, FC, AD, CSB, KEB, DJZ.

References

Alden, CB, **Coburn, SC**, **Wright, RJ**, **Baumann, E**, **Cossel, K**, **Perez, E**, **Hoenig, E**, **Prasad, K**, **Coddington, I**, **Rieker, GB**. 2019. Single-blind quantification of natural gas leaks from 1 km distance using frequency

combs. *Environmental Science & Technology* **53**(5): 2908–2917. DOI: https://dx.doi.org/10.1021/acs.est.8b06259.

Alden, CB, **Ghosh, S**, **Coburn, S**, **Sweeney, C**, **Karion, A**, **Wright, R**, **Coddington, I**, **Rieker, GB**, **Prasad, K**. 2018. Bootstrap inversion technique for atmospheric trace gas source detection and quantification using long open-path laser measurements. *Atmospheric Measurement Techniques* **11**(3): 1565–1582. DOI: https://dx.doi.org/10.5194/amt-11-1565-2018.

Allen, DT, **Pacsi, AP**, **Sullivan, DW**, **Zavala-Araiza, D**, **Harrison, M**, **Keen, K**, **Fraser, MP**, **Daniel Hill, A**, **Sawyer, RF**, **Seinfeld, JH**. 2015. Methane emissions from process equipment at natural gas production sites in the United States: Pneumatic Controllers. *Environmental Science & Technology* **49**(1): 633–640. DOI: https://dx.doi.org/10.1021/es5040156.

Allen, DT, **Torres, VM**, **Thomas, J**, **Sullivan, DW**, **Harrison, M**, **Hendler, A**, **Herndon, SC**, **Kolb, CE**, **Fraser, MP**, **Hill, AD**, **Lamb, BK**, **Miskimins, J**, **Sawyer, RF**, **Seinfeld, JH**. 2013. Measurements of methane emissions at natural gas production sites in the United States. *Proceedings of the National Academy of Sciences* **110**(44): 17768–17773. DOI: https://dx.doi.org/10.1073/pnas.1304880110.

Bell, CS, **Vaughn, T**, **Zimmerle, D**. 2020. Evaluation of next generation emission measurement technologies under repeatable test protocols. *Elementa: Science of the Anthropocene* **8**(1): 32. DOI: https://dx.doi.org/10.1525/elementa.426.

Bell, CS, **Vaughn, TL**, **Zimmerle, D**, **Herndon, SC**, **Yacovitch, TI**, **Heath, GA**, **Pétron**, **G**, **Edie, R**, **Field, RA**, **Murphy, SM**, **Robertson, AM**, **Soltis**, **J**. 2017. Comparison of methane emission estimates from multiple measurement techniques at natural gas production pads. *Elementa: Science of the Anthropocene* **5**(0): 79. DOI: https://dx.doi.org/10.1525/elementa.266.

Busse, AD, Zimmerman, JR. 1973. *User's guide for the climatological dispersion model*. Research Triangle Park, NC: National Environmental Research Center, Office of Research and Development, U.S. Environmental Protection Agency.

Chambers, A. 2003 Nov 19. *Well test flare plume monitoring: Results of DIAL measurements in Alberta*. Calgary, Canada: Petroleum Technology Alliance Canada: 1–48. The PTAC Air Issues Research Forum: Research priorities, discussion, and networking reception. Available at: https://www.osti.gov/etdeweb/biblio/20434087. Accessed 23 December 2021.

Clements, AL, **Griswold, WG**, **Abhijit, RS**, **Johnston, JE**, **Herting, MM**, **Thorson, J**, **Collier-Oxandale, A**, **Hannigan, M**. 2017. Low-cost air quality monitoring tools: From research to practice (a workshop summary). *Sensors* **17**(11): 2478. DOI: https://dx.doi.org/10.3390/s17112478.

Collier-Oxandale, A, **Hannigan, MP**, **Casey, JG**, **Piedrahita, R**, **Ortega, J**, **Halliday, H**, **Johnston, J**. 2018 Jan 12. Assessing a low-cost methane sensor quantification system for use in complex rural and urban environments. *Atmospheric Measurement Techniques Discussions* 1–35. DOI: https://dx.doi.org/10.5194/amt-2017-421.

Colorado Department of Public Health and Environment. 2021a. Regulation Number 7. Control of Ozone via Ozone Precursors and Control of Hydrocarbons via Oil and Gas Emissions (Emissions of Volatile Organic Compounds and Nitrogen Oxides). Available at https://cdphe.colorado.gov/aqcc-regulations. Accessed 15 March 2022.

Colorado Department of Public Health and Environment. 2021b Apr. Approved Instrument Monitoring Method (AIMM) for oil & gas. Available at https://cdphe.colorado.gov/oil-and-gas-and-your-health/approved-instrument-monitoring-method-aimm-for-oil-gas. Accessed 15 March 2022.

Colorado Oil and Gas Conservation Commission. 2020. Safety Regulations Series 600. Available at https://cogcc.state.co.us/documents/reg/Rules/LATEST/600Series.pdf. Accessed 26 August 2020.

Conley, S, **Faloona, I**, **Mehrotra, S**, **Suard, M**, **Lenschow, DH**, **Sweeney, C**, **Herndon, S**, **Schwietzke, S**, **Pétron, G, Pifer, J**, **Kort, EA**, **Schnell, R.** 2017. Application of Gauss's theorem to quantify localized surface emissions from airborne measurements of wind and trace gases. *Atmospheric Measurement Techniques* **10**(9): 3345–3358. DOI: https://dx.doi.org/10.5194/amt-10-3345-2017.

Duren, RM, **Thorpe, AK**, **Foster, KT**, **Rafiq, T**, **Hopkins, FM**, **Yadav, V**, **Bue, BD**, **Thompson, DR**, **Conley, S**, **Colombi, NK**, **Frankenberg, C**, **McCubbin, IB**, **Eastwood, ML**, **Falk, M**, **Herner, JD**, **Croes, BE**, **Green, RO**, **Miller, CE**. 2019. California's methane super-emitters. *Nature* **575**(7781): 180–184. DOI: https://dx.doi.org/10.1038/s41586-019-1720-3.

Edie, R, **Robertson, AM**, **Field, RA**, **Soltis, J**, **Snare, DA**, **Zimmerle, D**, **Bell, CS**, **Vaughn, TL**, **Murphy, SM**. 2020. Constraining the accuracy of flux estimates using OTM 33A. *Atmospheric Measurement Techniques* **13**(1): 341–353. DOI: https://dx.doi.org/10.5194/amt-13-341-2020.

Environmental Protection Agency. 2021. Leak detection and repair: A best practices guide. Available at https://www.epa.gov/sites/default/files/2014-02/documents/ldarguide.pdf. Accessed 15 March 2022.

Eugster, W, **Kling, GW**. 2012. Performance of a low-cost methane sensor for ambient concentration measurements in preliminary studies. *Atmospheric Measurement Techniques* **5**(8): 1925–1934. DOI: https://dx.doi.org/10.5194/amt-5-1925-2012.

The European Union. 2021. The New EU Methane Strategy. Available at https://www.europarl.europa.eu/legislative-train/theme-a-european-green-deal/file-methane-strategy/09-2021. Accessed 21 January 2020.

Flesch, TK, **Harper, LA**, **Powell, JM**, **Wilson, JD**. 2009. Inverse-dispersion calculation of ammonia emissions from Wisconsin dairy farms. *Transactions of the*

ASABE **52**(1): 253–265. DOI: https://dx.doi.org/10.13031/2013.25946.

Flesch, TK, **Wilson, J**, **Harper, L**, **Crenna, B**. 2005. Estimating gas emissions from a farm with an inverse-dispersion technique. *Atmospheric Environment* **39**(27): 4863–4874. DOI: https://dx.doi.org/10.1016/j.atmosenv.2005.04.032.

Flesch, TK, **Wilson, JD**, **Yee**, **E**. 1995. Backward-time Lagrangian stochastic dispersion models and their application to estimate gaseous emissions. *Journal of Applied Meteorology and Climatology* **34**(6): 1320–1332. Boston, MA: American Meteorological Society. DOI: https://dx.doi.org/10.1175/1520-0450(1995)034<1320:BTLSDM>2.0.CO;2.

Johnson, MR, **Kostiuk, LW**. 2002. A parametric model for the efficiency of a flare in crosswind. *Proceedings of the Combustion Institute* **29**(2): 1943–1950. DOI: https://dx.doi.org/10.1016/S1540-7489(02)80236-X.

Johnson, MR, **Tyner, DR**, **Conley, S**, **Schwietzke, S**, **Zavala-Araiza, D**. 2017. Comparisons of airborne measurements and inventory estimates of methane emissions in the Alberta upstream oil and gas sector. *Environmental Science & Technology* **51**(21): 13008–13017. DOI: https://dx.doi.org/10.1021/acs.est.7b03525.

Lamb, BK, **McManus, JB**, **Shorter, JH**, **Kolb, CE**, **Byard, M**, **Harriss, RC**, **Allwine, E**, **Denise, B**, **Touche, H**, **Alex, G**, **Lott, RA**, **Siverson, R**, **Westburg, H**, **Zimmerman, P**. 1995. Development of atmospheric tracer methods to measure methane emissions from natural gas facilities and urban areas. *Environmental Science & Technology* **29**(6): 1468–1479. DOI: https://dx.doi.org/10.1021/es00006a007.

Laubach, J, Kelliher, FM, Knight, TW, Clark, H, Molano, G, Cavanagh, A. 2008. Methane emissions from beef cattle. *Australian Journal of Experimental Agriculture* **48**: 132e137. DOI: https://dx.doi.org/10.1071/EA07256.

Log, T, **Pedersen, WB**, **Moumets, H**. 2019. Optical Gas Imaging (OGI) as a moderator for interdisciplinary cooperation, reduced emissions and increased safety. *Energies* **12**(8): 1454. DOI: https://dx.doi.org/10.3390/en12081454.

Morawska, L, **Thai, PK**, **Liu, X**, **Asumadu-Sakyi, A**, **Ayoko, G**, **Bartonova, A**, **Bedini, A**, **Chai, F**, **Christensen, B**, **Dunbabin, M**, **Gao, J**, **Hagler**, **GSW**, **Jayaratne, R**, **Kumar, P**, **Lau, AKH**, **Louie, PKK**, **Mazaheri, M**, **Ning, Z**, **Williams, R**. 2018. Applications of low-cost sensing technologies for air quality monitoring and exposure assessment: How far have they gone? *Environment International* **116**: 286–299. DOI: https://dx.doi.org/10.1016/j.envint.2018.04.018.

Okorn, K, **Jimenez, A**, **Collier-Oxandale, A**, **Johnston, J**, **Hannigan, M**. 2021. Characterizing methane and total non-methane hydrocarbon levels in Los Angeles communities with oil and gas facilities using air quality monitors. *Science of the Total Environment* **777**: 146194. DOI: https://dx.doi.org/10.1016/j.scitotenv.2021.146194.

Pacsi, AP, **Ferrara, T**, **Schwan, K**, **Tupper, P**, **Lev-On, M**, **Smith, R**, **Ritter, K**. 2019. Equipment leak detection and quantification at 67 oil and gas sites in the Western United States. *Elementa: Science of the Anthropocene* **7**(1): 29. DOI: https://dx.doi.org/10.1525/elementa.368.

Pasquill, F. 1975. Limitations and prospects in the estimation of dispersion of pollution on a regional scale, in *Advances in geophysics*. Amsterdam, The Netherlands: Elsevier: 1–13. DOI: https://dx.doi.org/10.1016/S0065-2687(08)60568-3.

Pasquill, F, **Smith, FB**. 1983. *Atmospheric diffusion* (Vol. 110). 3rd edition. Hoboken, NJ: Ellis Horwood (John Wiley & Sons). Available at http://doi.wiley.com/10.1002/qj.49711046416. Accessed 8 May 2019.

Peterson, H, **Lamb**, **B**. 1992. Comparison of results from a meandering-plume model with measured atmospheric tracer concentration fluctuations. *Journal of Applied Meteorology and Climatology* **31**(6): 553–564. DOI: https://dx.doi.org/10.1175/1520-0450(1992)031<0553:CORFAM>2.0.CO;2.

Riddick, SN, **Ancona, R**, **Bell CS**, **Duggan, A**, **Vaughn, TL**, **Bennett, K**, **Zimmerle, DJ**. 2022. Quantitative comparison of methods used to estimate methane emissions from small point sources. *Atmospheric Measurement Techniques Discussion.* DOI: https://doi.org/10.5194/amt-2022-9.

Riddick, SN, **Mauzerall, DL**, **Celia, M**, **Allen, G**, **Pitt, J**, **Kang, M**, **Riddick, JC**. 2020. The calibration and deployment of a low-cost methane sensor. *Atmospheric Environment* 117440. DOI: https://dx.doi.org/10.1016/j.atmosenv.2020.117440.

Seinfeld, JH, **Pandis, SN**. 2016. *Atmospheric chemistry and physics: From air pollution to climate change*. 3rd edition. Hoboken, NJ: John Wiley & Sons, Inc.

Shamasunder, B, **Collier-Oxandale, A**, **Blickley, J**, **Sadd, J**, **Chan, M**, **Navarro, S**, **Hannigan, M**, **Wong, NJ**. 2018. Community-based health and exposure study around urban oil developments in South Los Angeles. *International Journal of Environmental Research and Public Health* **15**(1): 138. DOI: https://dx.doi.org/10.3390/ijerph15010138.

Sonderfeld, H, **Bösch, H**, **Jeanjean, APR**, **Riddick, SN**, **Allen, G**, **Ars, S**, **Davies, S**, **Harris, N**, **Humpage, N**, **Leigh, R**, **Pitt, J**. 2017. CH_4 emission estimates from an active landfill site inferred from a combined approach of CFD modelling and in situ FTIR measurements. *Atmospheric Measurement Techniques* **10**(10): 3931–3946. DOI: https://dx.doi.org/10.5194/amt-10-3931-2017.

U.S. Environmental Protection Agency. 1995. *Industrial Source Complex (ISC3) Dispersion Model*. Research Triangle Park, NC: U.S. Environmental Protection Agency. User's Guide. EPA 454/B 95 003a (Vol. I) and EPA 454/B 95 003b (Vol. II).

Vaughn, TL, **Bell, CS**, **Yacovitch, TI**, **Roscioli, JR**, **Herndon, SC**, **Conley, S**, **Schwietzke, S**, **Heath, GA**, **Pétron**, **G**, **Zimmerle**, **D**. 2017. Comparing facility-level

methane emission rate estimates at natural gas gathering and boosting stations. *Elementa: Science of the Anthropocene* **5**: 71. DOI: https://dx.doi.org/10.1525/elementa.257.

World Bank Group. 2013. *Guidance on upstream flaring and venting: Policy and regulation (English)*. Global Gas Flaring Reduction (GGFR) Washington, DC: World Bank Group. Available at http://documents.worldbank.org/curated/en/200701468344636937/Guidance-on-upstream-flaring-and-venting-policy-and-regulation. Accessed 28 December 2021.

World Bank Group. 2021. *Regulation of associated gas flaring and venting: A global overview and lessons from international experience (English)*. Global gas flaring reduction: A public-private partnership: No. 3 Washington, DC: World Bank Group. Available at https://documents1.worldbank.org/curated/ar/590561468765565919/pdf/295540Regulati1aring0no10301public1.pdf. Accessed 28 December 2021.

Zavala-Araiza, D, **Omara, M**, **Gautam, R**, **Smith, ML**, **Pandey, S**, **Aben, I**, **Almanza-Veloz, V**, **Conley, S**, **Houweling, S**, **Kort, EA**, **Maasakkers, JD**, **Molina, LT**, **Pusuluri, A**, **Scarpelli, T**, **Schwietzke, S**, **Shen, L**, **Zavala, M**, **Hamburg, SP**. 2021. A tale of two regions: Methane emissions from oil and gas production in offshore/onshore Mexico. *Environmental Research Letters* **16**(2): 024019. DOI: https://dx.doi.org/10.1088/1748-9326/abceeb.

Zimmerle, D, **Vaughn, T**, **Bell, C**, **Bennett, K**, **Deshmukh, P**, **Thoma, E**. 2020. Detection limits of optical gas imaging for natural gas leak detection in realistic controlled conditions. *Environmental Science & Technology* **54**(18): 11506–11514. DOI: https://dx.doi.org/10.1021/acs.est.0c01285.

How to cite this article: Riddick, SN, Ancona, R, Cheptonui, F, Bell, CS, Duggan, A, Bennett, KE, Zimmerle, DJ. 2022. A cautionary report of calculating methane emissions using low-cost fence-line sensors. *Elementa: Science of the Anthropocene* 10(1). DOI: https://doi.org/10.1525/elementa.2022.00021

Domain Editor-in-Chief: Detlev Helmig, Boulder AIR LLC, Boulder, CO, USA

Guest Editor: Brian Lamb, Washington State University, Pullman, WA, USA

Knowledge Domain: Atmospheric Science

Part of an Elementa Forum: Oil and Natural Gas Development: Air Quality, Climate Science, and Policy

Published: May 27, 2022 **Accepted:** April 28, 2022 **Submitted:** February 2, 2022

ELEMENTA Science of the Anthropocene

Elem Sci Anth is a peer-reviewed open access journal published by University of California Press.

OPEN ACCESS